NASA Technical Memorandum 105438

Influence of Engineered Interfaces on Residual Stresses and Mechanical Response in Metal Matrix Composites

Steven M. Arnold
Lewis Research Center
Cleveland, Ohio

and

Thomas E. Wilt
University of Toledo
Toledo, Ohio

March 1992

NASA

INFLUENCE OF ENGINEERED INTERFACES ON RESIDUAL STRESSES AND MECHANICAL RESPONSE IN METAL MATRIX COMPOSITES

by

S. M. Arnold
National Aeronautics and Space Administration
Lewis Research Center
Cleveland, Ohio

and

T. E. Wilt
University of Toledo
Toledo, Ohio

ABSTRACT

Because of the inherent coefficient of thermal expansion (CTE) mismatch between fiber and matrix within metal and intermetallic matrix composite systems, high residual stresses can develop under various thermal loading conditions. These conditions include cooling from processing temperature to room temperature as well as subsequent thermal cycling. As a result of these stresses, within certain composite systems, radial, circumferential, and/or longitudinal cracks have been observed to form at the fiber–matrix interface region. A number of potential solutions for reducing this thermally induced residual stress field have been proposed recently. Examples of some potential solutions are high CTE fibers, fiber preheating, thermal anneal treatments and an engineered interface (e.g., a compensating/compliant layer concept or a graded layer concept). In the strict sense, an engineered interface is one that provides a compromise between the various pertinent chemistry and mechanics issues for the application and the system under consideration. Here, the focus is on designing an interface (by using a compensating/compliant layer concept) to reduce or eliminate the thermal residual stress field and, therefore, the initiation and propagation of cracks developed during thermal loading. Furthermore, the impact of the engineered interface on the composite's mechanical response when subjected to isothermal mechanical load histories is examined.

INTRODUCTION

Metal and intermetallic matrix composites are currently being considered for advanced aerospace applications because of their attractive high strength–to–density ratio. However, the inherent coefficient of thermal expansion (CTE) mismatch between fiber and matrix causes high residual stresses to develop in these composite systems under various thermal load histories. Such conditions include cooling from the processing consolidation temperature to room temperature as well as subsequent thermal cycling. These stresses may be of sufficient magnitude to generate radial, circumferential (interfacial debonding), and/or longitudinal cracks within the matrix or fiber/matrix interface region. For example, in the case of SiC/Ti_3Al+Nb and SiC/Ti–15–3 systems, microscopic radial

cracks, which have been observed at the fiber–matrix interface after fabrication, proliferate after thermal cycling [1]. In addition to radial cracks, other (less frequently observed) crack orientations are illustrated schematically in figure 1.

A number of potential solutions for reducing this thermally induced residual stress field have been proposed recently. Examples of some potential solutions are high CTE fibers, fiber preheating, thermal anneal treatments and engineered interfaces (e.g., compensating/compliant layers or a graded layer concept). In the strict sense, an engineered interface is one that provides a compromise between the various pertinent chemistry and mechanics issues for the application and system under consideration. For example, the choice of a coating material for a given fiber/matrix combination will first be based on its ability to act as a chemical barrier between the fiber and matrix. However, an ideal coating should also, besides inhibiting fiber/matrix reactions, cause a reduction in thermal residual stresses at the fiber/matrix interface and, if possible, within the system as a whole. An additional advantage may be its ability to act as a crack–blunting layer to minimize crack propagation.

Here, as a result of previous work [2,3] which will be highlighted subsequently, two types of engineered interfaces are put forth to reduce or eliminate the initiation of cracks developed during cooldown and subsequent use in the SiC/Ti_3Al+Nb system; the first, a compliant layer concept, is an interface (e.g., Nb) that will increase or maintain the ductility at the fiber/matrix interface, but will not necessarily reduce the residual stresses within the system. It does this by acting as a diffusion barrier which minimizes, if not eliminates, chemical reactions leading to the formation of a brittle layer. The second, a compensating layer concept, is an interface (e.g., Cu/Nb) that not only will act as a compliant layer but also will reduce the residual stresses within the system, because its CTE is higher than that of the matrix.

The objective of the present paper is to study the influence of these two types of engineered interfaces on the composite's residual stress state after fabrication and on its mechanical response when subsequently subjected to both thermal and mechanical load histories. The stress analysis employed can be divided into two parts. The first, an elastic–plastic axisymmetric concentric cylinder model that does not account for any surrounding fiber interaction, was employed to investigate the thermal response of the composite. The second, a three–dimensional elastic–plastic unit cell model with periodic boundary conditions representing a hexagonally packed composite architecture, was employed to analyze the mechanical response of the various composite systems. Clearly, in order to accurately predict both residual stresses and subsequent thermal and mechanical response, both the interface layer and matrix should be considered to behave

viscoplastically (i.e., be rate dependent). However, this additional level of complexity is purposely avoided here by assuming there is a stress–free temperature (below the consolidation temperature) below which the material behaves as a rate independent elastic – plastic material. The chemical compatibility issues for these two interface concepts have been previously addressed by Misra [4,5].

This paper begins by summarizing the major results of the previous studies leading to the selection of these two interface materials (Nb and Cu) for the SiC/Ti_3Al+Nb system. Then a brief description of the stress analysis conducted and material properties used is given, followed by fabrication, thermal cycling, and longitudinal and transverse mechanical load stress analysis results. It is important to remember that the objective of the present analysis is to provide qualitative insight into the behavior of composites with engineered (compliant/compensating) interfaces rather than to make any quantitative assessment of performance.

BACKGROUND

Previous work conducted by Arnold et.al. [2] devoted significant effort to understanding and describing the mechanics of the problem, specifically, the importance of the initial stress analysis assumptions and the desired characteristics of an interface layer (i.e., thickness and thermomechanical properties) that will minimize the local tensile residual stresses (principally the hoop stress) within the system and, thereby, reduce the tendency toward cracking. Conclusions were obtained by performing a detailed parametric study by a finite element concentric cylinder model with generalized plane strain end conditions and free boundary conditions. The fiber, SiC, was assumed to be isotropic and linear elastic, whereas the unknown interface layer and matrix (Ti_3Al+Nb) cylinders were assumed to be isotropic and bilinear elastic–plastic. The unknown interface layer properties were normalized with respect to the corresponding known matrix properties over the full temperature range. Finally, perfect bonding between cylinders was assumed, and only the initial cooldown cycle was analyzed.

Within the confines of these assumptions, calculations have shown that the CTE and thickness of an interface material inserted between the fiber and matrix dominate when an attempt is made to reduce or eliminate in–plane fiber and matrix residual stresses and, therefore, radial cracking. More specifically, increasing the CTE (α) and thickness (t) of the interface layer decreases the in–plane stress (σ_r,σ_θ) within the fiber and matrix while increasing the out–of–plane (σ_z) stress component, thus potentially initiating longitudinal cracking. If interface bonding were strictly frictional, the reduction in radial

stress due to the addition of an interface layer could be extremely detrimental to the overall composite performance.

Conversely, the mechanical properties of the interface (i.e., yield point σ_y^I, hardening slope H^I, and stiffness E^I) dominate when an attempt is made to reduce the stress state within the interface layer, and *yet they have little if any effect* on the fiber or matrix stress state. Furthermore, it has been observed that when an interface layer material is selected, the following properties should be chosen:

(1) $\alpha^I > \alpha^m$, for a compensating type interfacial layer

or

$\alpha^f < \alpha^I < \alpha^m$, for a compliant type interfacial layer

(2) t/a is as large as other considerations allow (a is the fiber radius)

(3) $H^I/H^m + \sigma_y^I/\sigma_y^m$ is small

(4) Yield point σ_y^I is low relative to that of the matrix (σ_y^m)

(5) Hardening slope H^I is low relative to that of the matrix (H^m)

(6) Elastic stiffness E^I is low relative to that of the matrix (E^m)

where the superscript m and I indicate matrix and interface respectively. The preceding list is in order of importance, with respect to impact, for obtaining a required minimum overall residual stress state. Be aware, however, that this requirement may not provide maximum life under cyclic conditions. In fact, in a recent study [6] shakedown was utilized to assess the effectiveness of an interface in improving the low cycle fatigue of the composite when it was subjected to thermal cycles and transverse loading; the study showed that in order to insure shakedown it is desirable to have a high yield stress in the layer. The inclusion of plasticity has also been shown [2,6] to significantly influence the actual magnitude and distribution of stress (i.e., the resulting trends); and therefore, it must be included in the analysis.

Given the above material parameter guidelines and other bounds on key parameters [2] (e.g., $\alpha^I/\alpha^m > 1.2$, and $0.1 < t/a < 0.2$), which were obtained by calibrating the analysis with an interface to one without an interface, candidate pure element and alloy interface materials (i.e., compliant, compensating, and/or diffusion barrier materials) were put forth. As a result of thermodynamic studies [5,7] conducted on the various candidate materials, Nb and Cu were chosen to represent a compliant layer interface and a compensating layer interface, respectively. Note that in the case of the Cu interface, an additional diffusion barrier (in this case, Nb) was shown to be needed between

the Cu and the Ti_3Al+Nb matrix because of chemical incompatibilities [5]. In a recent study Misra and Arnold [4], using a single SCS–6 fiber hot pressed between two disks of Ti_3Al as the control and another single SCS–6 fiber hot pressed between two Nb–clad Ti_3Al disks as the test, showed that a Nb compliant layer was effective in reducing radial cracks even though the residual stress state was shown analytically not to be greatly reduced. The success in preventing radial cracking is primarily attributable to the increased ductility and minimized reaction zone due to the presence of the Nb.

Currently, Textron Specialty Materials, Inc., is under contract with NASA Lewis to manufacture both the Nb and Cu/Nb systems in unidirectional plate form in order to investigate and verify, experimentally, the applicability of employing either a compliant or compensating layer technology. The present paper constitutes an analytical study of these two specific systems.

STRESS ANALYSIS

All stress analyses were performed numerically with the nonlinear finite element program MARC [8] and can be divided into two parts. Part one employed an axisymmetric finite element concentric cylinder model to investigate the residual stresses developed during cooldown from consolidation, as well as the change in stress state due to subsequent thermal cycling. The concentric cylinder model (shown in fig. 2) consists of a single fiber (of radius a) embedded in coaxial cylindrical shells of an interface material(s) (outer radius b) and matrix material (outer radius c). Owing to the obvious cylindrical symmetry, the problem is expressed in cylindrical polar coordinates r, θ, and z. Figure 2 also illustrates the generalized plane strain and axisymmetric finite element boundary conditions imposed on the r–z plane. Each cylinder was assumed to be composed of a homogeneous isotropic material and perfect bonds between fiber, interface, and matrix was assumed. Even though this model did not account for surrounding fiber interactions and because the problem was thermal in nature and only thermal loading histories were examined, the effect of fiber volume fraction (v_f) could easily be studied, since $v_f = a^2/c^2$.

Part two of the analysis employed a three–dimensional unit cell model, with periodic boundary conditions (shown in fig. 3) representing a hexagonally packed composite architecture, to investigate the mechanical response of a composite ($v_f = 35\%$) subjected to both longitudinal and transverse loading. Here both the case of no bonding and that of perfect bonding between fiber and nonfiber material are examined.

Throughout the stress analysis, temperature dependent constituent material properties were utilized. The incorporation of yielding (or plasticity) was accomplished by assuming a uniaxial bilinear stress–strain response of both the matrix and interface materials and a von Mises multiaxial yield criterion. The temperature–dependent material response determined experimentally by Brindley [9,10] for the Ti_3Al+Nb matrix clearly supports this assumption. Table I summarizes these temperature–dependent elastic and/or plastic properties used in the analysis for the SCS–6 fiber and the Ti_3Al+Nb matrix [9 to 11]; Tables II and III summarize the temperature–dependent properties used for Nb and Cu, respectively [12 to 14]. Note that engineering judgment has been used when assigning difficult–to–obtain material property data. For example, in the case of Nb, the hardening modulus was taken as one–quarter that of Cu.

RESULTS: PART I – THERMAL RESPONSE

Thermal Residual Stresses

Let us begin by examining the residual stresses resulting from cooldown from a stress free temperature (lower than that of consolidation) to room temperature (i.e., $\Delta T = -1425^\circ F$ or $-774^\circ C$). The concentric cylinder model is used with a fiber volume ratio of 40%, and when applicable, a normalized interfacial layer thickness (t/a) of 0.1. Note: "a" is defined to be the fiber radius (see fig. 2). Figures 4 to 6 show the principal stress components σ_r, σ_θ, and σ_z, respectively, versus the normalized radial location (r/a) within the concentric cylinder model, for the case with no interface layer, F/M (SCS–6/Ti_3Al+Nb); and the cases with an interface layer, that is, F/Nb/M (SCS–6/Nb/Ti_3Al+Nb), F/Cu/M (SCS–6/Cu/Ti_3Al+Nb), and F/Cu/Nb/M (SCS–6/Cu/Nb/Ti_3Al+Nb).

From examination of figures 4 to 6, a number of observations can be made about the effectiveness of the two interface concepts. For example, in the case of the compliant layer concept (F/Nb/M), no significant reduction is observed in the residual stress components (σ_r,σ_θ or σ_z) in the fiber and matrix materials over those of the F/M system. However, both the circumferential (σ_θ) and axial (σ_z) stresses within the Nb interface layer itself are significantly less than those in the F/M system just beyond the OR (outer radius) of the fiber. To assess the importance of these stress levels within the Nb, relative to initiation of radial and axial cracks, one must examine the various failure criteria and parameters for this material; such an examination however, is beyond the scope of the present study.

In the case of the compensating layer concept (i.e., F/Cu/M and F/Cu/Nb/M) it is clear that reductions are achieved in both the radial (σ_r) and circumferential (σ_θ) stress components within the fiber and matrix materials, as compared to those of the F/M

system; while an increase in the axial (σ_z) component is achevied, as expected from work [2] described previously. Note that in the F/Cu/Nb/M system, which is being manufactured by Textron, the inclusion of a thin layer of Nb as a diffusion barrier slightly reduced the effectiveness of the Cu layer (fig. 5). Furthermore, in both concepts, the in–plane stresses are the dominantly affected ones, with reductions in the range of 15 to 40% (depending upon radial location) whereas the axial (out–of–plane) component is basically unaffected (less than 5%).

Figure 7 shows the effective stress[1] ($\bar{\sigma} = \sqrt{3J_2}$; $J_2 = 1/2\ S_{ij}S_{ij}$; and $S_{ij} = \sigma_{ij} - 1/3\sigma_{kk}\delta_{ij}$) versus temperature at location b' in the matrix (r/a = 1.1, see fig. 5) for all cases; it clearly indicates the temperature at which yielding (plasticity) initiates in the matrix. This temperature may be defined as the "plastic temperature". For the cases of F/M and F/Nb/M, this plastic temperature is approximately 302° C whereas for the cases of F/Cu/M and F/Cu/Nb/M, it is 190.5° C. Thus the compliant layer concept (F/Nb/M) does not lower the plastic temperature relative to that of the F/M system, but the compensating layer concept (F/Cu/M) does modify the plastic temperature by approximately 93° C, because of a reduction in the effective stress state. Note that in the F/M case, the plastic temperature is taken as the temperature at which the plastic zone reaches the radial location b', given by r/a=1.1, and not that at which first yielding occurs at the matrix IR (inner radius), which is approximately 316° C.

Similarly, figure 8 shows the effective stress versus temperature at the IR and OR of the interface (whether Cu or Nb) and, thus, the temperature at which yielding occurs in the interface. Clearly, since the Cu layer initially has a lower yield point than does Nb, the plastic temperature is of course higher, 743 versus 643° C, respectively. Therefore, in summary, the insertion of a Cu layer results in an increased elastic temperature zone within the matrix during cooling, because of the reduction in thermal stress buildup, due primarily to the CTE of the interface being greater than that of the matrix. Also one can observe that hardening in the Cu interface is significant, whereas hardening in the Nb is merely keeping pace with the change in yield stress due to a change in temperature. Finally, note that at room temperature the Cu interface has a significant stress gradient (i.e., IR > OR), but that of the Nb interface does not (see fig. 9).

---

[1]The effective stress [15], sometimes referred to as the equivalent stress [16], is a scalar function representing the second invariant (J_2) of the mulitiaxial devatoric stress components (S_{ij}), for the von Mises yield criterion; thus yielding occurs when the effective (equivalent) stress reaches the tensile yield strength (σ_y) of the material.

Effect of Layer Thickness

As indicated by previous work [2,3], the thickness of the interfacial layer also plays a major role in modifying the residual stress state. This thickness dependence is illustrated by comparing figures 9 and 5, both of which show the principal stress component (σ_θ) versus normalized radial location for all cases under consideration, but the interface thickness (0.1 in fig. 5) is increased to 0.2 (see fig. 9). Notice that the effectiveness of the Cu layer is increased dramatically, in that a 64 % decrease in matrix stress (fig. 9) over the previous 18 % reduction (fig. 5) at the matrix IR is achieved; whereas the matrix stress is only slightly increased with the use of the Nb layer. In a similar way, the impact of including a relatively thin Nb diffusion barrier in addition to the Cu compensating layer is illustrated in figure 10. Here it is shown that as the thickness of the Cu layer is increased relative to the Nb coating (which is held constant at t/a=0.05) the overall effectiveness of the compensating layer is increased; that is, the matrix and fiber stresses are decreased. Thus, henceforth only the F/M , F/Nb/M and F/Cu/M cases will be studied since the F/Cu/Nb/M system's behavior can be expected to be comparable to that of the F/Cu/M system. As a final observation, note that when the Cu thickness is at least twice that of the Nb, the Nb layer is put into a state of compression (fig. 9), thus potentially increasing its ability to either resist cracking or blunt an advancing crack.

Effect of Fiber Volume Fraction

Before moving on to examine the impact of compensating and compliant layers on the thermal cycling response of composites, let us consider another important factor that influences the buildup of residual stresses, fiber volume fraction. This influence is illustrated in figures 11 to 13, where the principal stresses (σ_r, σ_θ, and σ_z, respectively) versus percent fiber volume ratio are shown. These stresses correspond to those developed at the matrix IR (location b', fig. 5) during cooldown to room temperature, and for t/a=0.1 when applicable.

Considering the case in which no interface layer is present (i.e., F/M), one observes that the radial clamping stress increases with decreasing fiber volume ratio, whereas the circumferential and axial stress decrease. In fact, when the volume fraction is below 8% (see fig. 13) the axial stress in the matrix becomes negative because of the insufficient constraint offered by the fibers.

Inclusion of a compliant layer (i.e., Nb) modifies the magnitude of the residual stress, but clearly does not alter the influence of the fiber volume ratio; that is, the clamping radial stress still increases with decreasing volume fraction whereas σ_θ and σ_z decrease. Note, however, that for all volume fractions the circumferential and axial

residual stress is increased over that of the F/M system alone and that the axial stress remains tensile.

Alternatively, inclusion of a compensating layer (i.e.,Cu) not only significantly modifies the resulting magnitude of the residual stress developed, but also alters the influence of the fiber volume ratio, particularly with respect to the σ_θ stress component. For example, in figure 12 one can see that for fiber volumes greater than 25 %, σ_θ is increasingly reduced over that of the F/M case and that an apparent plateau is reach below a volume fraction of 25%, such that σ_θ actually increases above that of the F/M case. The reason for such a plateau is not fully understood at this time. However, it is known that the stress level as well as fiber volume ratio at which this plateau occurs is dependent upon the thickness of the compensating layer, that is, for a thicker layer the (F/Cu/M) circumferential stress drops below that of the (F/M). Furthermore, this plateau is thought to be associated with the occurrence of a fully compressive state of stress (and therefore a decrease in plasticity) within the compensating layer itself, below a 25% volume fraction, as illustrated in figures 14 and 15. Figures 14 and 15 also illustrate the fact that the magnitude of the circumferential and axial stress in the Cu is less than that in the Nb for all fiber volumes. Figures 11 through 15 illustrate an important difference between selecting a compensating layer over a compliant layer, in that one can produce higher fiber volume fractions and still maintain the same level of matrix residual stress as that in the F/M case at a lower volume fraction. In addition these results illustrate the importance of considering more than one volume fraction when attempting to verify these compensating/compliant layer concepts.

Thermal Cycles

Let us return to a fiber volume fraction of 40% and examine, with the concentric cylinder model, the stress–strain response of the various systems when they are subjected to a full thermal cycle, that is, cooldown from the initial stress–free temperature (B) to room temperature 23° C or 75° F (RT) and back up to the previous stress–free temperature (H), of 815° C (or 1500° F). Points B, RT, and H as well as the entire effective stress–effective mechanical strain ($\bar{\sigma} - \bar{\epsilon}$) history, assuming a von Mises isotropic hardening model [15], are shown in figure 16 for the F/M, F/Cu/M, and F/Nb/M systems. Note that these stress and strain values are obtained at location b' in the matrix (fig. 5), and that $\bar{\sigma} = \sqrt{3J_2}$, $\bar{\epsilon} = \sqrt{3\mathcal{J}_2}$, $\mathcal{J}_2 = 1/2\ \epsilon_{ij}\epsilon_{ij}$, and $\epsilon_{ij} = e_{ij} - 1/3e_{kk}\delta_{ij}$, where e_{ij} is the total mechanical strain. It is important to realize that, with the present definition of effective

strain, the uniaxial stress–strain response would be related through the shear modulus and not Young's modulus.

From figure 16, one observes that again the F/M and F/Nb/M systems behave similarly and that the Cu interface within the F/Cu/M system greatly reduces the accumulated effective mechanical strain incurred in the matrix during cooldown to RT and, therefore, the amount of permanent set and residual compressive stress achieved on return to the maximum temperature (H). Monitoring the accumulation of plastic strain indicated that the heatup portion (RT to H) of the cycle (although nonlinear) is fully elastic in all three systems. The nonlinearity in the response can be primarily attributed to the temperature dependence of the associated material parameters.

As an aside, monitoring the plastic strains within the interface layers themselves, following cooldown, also indicated that in the Nb system an elastic interface response is produced from room temperature up to approximately 638° C, whereas in the Cu system, an elastic interface response is produced only up to 249° C. It is helpful to remember that, during the cooldown portion of the cycle, σ_r goes into compression while σ_θ and σ_z are tensile, and during the heat up portion, σ_r becomes tensile while σ_θ and σ_z are compressive.

Since isotropic hardening may not be completely realistic in that it cannot account for the Bauschinger effect exhibited by most structural materials, a von Mises plasticity model with kinematic hardening[15] is also considered. Note, an isotropic hardening rule is one that assumes the initial yield surface expands uniformly, without distortion or translation, as plastic flow occurs. In constrast, a kinematic hardening rule assumes that the initial yield surface translates as a rigid body (i.e., maintaining its original size, shape, and orientation). As a result, differences in response will be observed under load histories that involve stress reversals.

For example, in the initial cycle just described, identical effective stress and strain behavior is observed when the kinematic model is used. However, upon further cycling, a difference between isotropic (fig. 17) and kinematic hardening (fig. 18) can be seen. Most notable is the F/Cu/M system in that under isotropic hardening continued ratcheting occurs for all three imposed cycles, whereas with kinematic hardening shakedown occurs after the second cycle. Conversely, in the F/M and F/Nb/M systems, considering isotropic hardening, shakedown occurs after the first cycle, but with kinematic hardening two cycles are needed. An important observation relative to fatigue is that in all three systems the hysteresis loops have no widths, and only a small amount of plastic strain is incurred when ratcheting is present. Given this, one would expect the failure of the matrix material to be that of high cycle fatigue. Comparing the three systems, makes clear that the F/Cu/M

system gives rise to the smallest effective mechanical strain range and the F/Nb/M system, the largest, thereby suggesting that the compensating layer should provide the longest matrix life.

Figure 19 shows the associated effective stress versus effective mechanical strain history, occurring at the inner radius of the Nb interface, during the three imposed thermal cycles. Note that both isotropic and kinematic hardening produce essentially the same saturated hysteresis loops and that these loops have a finite width, thus indicating the potential for low cycle fatigue of the interface.

Figure 20 shows the effective stress – effective mechanical strain response occurring at the inner radius of the Cu interface and indicates a significant difference between isotropic and kinematic hardening assumptions. In the case of kinematic hardening the stress range remains comparatively small (i.e., approximately 207 MPa at the cold end and 69 MPa on the hot end of the cycle); in contrast, the total mechanical strain range is relatively large (on the order of 3%) and a limit cycle is reached after the first cycle. In the case of isotropic hardening no limit cycle is achieved within the three imposed cycles, and the stress range increases (on both the cold and hot ends of the cycle) while the strain range decreases per cycle. The predicted stress levels shown in figure 20 are somewhat higher than one might expect, given that cold–worked OFHC copper (1 hr at 104° C) has a yield strength of approximately 345 MPa; however, these inaccuracies can be attributed to the coarse characterization of each constituent's constitutive model. Also this overprediction suggests that the results not be used quantitatively but rather qualitatively, as initially intended by the authors.

In making a qualitative life assessment, the method of universal slopes[17] and the isothermal data for each material at the maximum temperature were utilized. By comparing the effective mechanical strain range incurred in the Cu layer (2.5%) to that in the Nb layer (0.625%), one would conclude that the Nb interface should last approximately three times longer than the Cu interface, even though the ductility of the Cu layer exceeds that of the Nb. Furthermore, examination of the individual component hysteresis loops (e.g., σ_r vs ϵ_r, or σ_θ vs ϵ_θ, or σ_z vs ϵ_z) suggests that radial cracking within the interfaces will be the dominate mode of damage accumulation. However, it is important to keep in mind that although the Cu interface is thought to experience crack initiation first, this does not ensure that the F/Cu/M composite system, as a whole, will experience failure first. As a result, final judgment must be postponed until experimental results are available to provide additional guidance.

A final comment relative to thermal cycling: both the interface and matrix materials should be used to their maximum capacity. Specifically, one should not design a

system such that the interface compensates so much that the interface itself fails prematurely to the matrix. How one might use (or design) the thickness of each individual layer in a multi–layered system, such as F/Cu/Nb/M, to minimize the residual stress within the matrix and yet not overstress and prematurely fail the interface layers themselves, can be inferred from figure 10.

RESULTS: PART II – MECHANICAL RESPONSE

Here, the mechanical response (e.g., longitudinal and transverse stress–strain curves) for the F/M, F/Cu/M, and F/Nb/M systems are examined. As stated earlier, a three–dimensional unit cell model with periodic boundary conditions representing a hexagonal packed composite architecture with a fiber volume of 35% was used.

Longitudinal Response

After the system was cooled down from a stress–free temperature (SFT) to room temperature (RT), an axial load was applied to the unit cell, and the axial strain was predicted. Figure 21 shows the longitudinal macro stress–strain (Σ_z–e_z) response at room temperature for systems without an interface layer (F/M) and with an interface layer, (F/Cu/M and F/Nb/M). Also, shown in figure 21 are the stress–strain responses for both the fiber and matrix constituents. Note that the constituent stress level is given by the vertical axis on the left, and the total (macro) stress applied to the composite is indicated by the vertical axis on the right. Overall, only a slight degradation in load carrying capability is observed with the inclusion of either interface as compared to the F/M only case. Initially, the F/Cu/M system response is similar to that of the F/M system, but at high magnitudes of stress and strain the F/Nb/M system responds more closely. As shown by experimental results [10] and as can be seen in figure 21, the entire longitudinal composite stress–strain curve can be represented by a bilinear curve, where the elastic limit of the composite is coincident with nonlocalized yielding of the matrix material. Also, experimental results [10] have shown the strain–to–failure of the composite (with v_f = 35%) to be 0.75% and the UTS to be 1210 MPa at 23°C. Note that the stress level in figure 21 corresponding to a tensile strain of 0.75% (see RT axis) or 0.3% (see SFT axis) is predicted to be 1207 MPa. As an aside, it has been shown that accounting for the residual compressive stress (–689 MPa), or the residual compressive mechanical strain (ϵ_z = –0.15%) within the fiber allows one to predict the required macro axial stress (or strain) needed to bring the fiber into a tensile state (see point A, fig. 21). Furthermore, given the statistical mean strain to failure of the fibers [18] within the composite , one can predict the UTS of the composite. For the above cases the macro stress (see point B, fig. 21) required to overcome the compressive residual strain in the fiber is approximately 290

MPa. Note that the residual compressive mechanical strain in the fiber can be approximated by taking the difference between the CTE of the composite and that of the fiber and multiplying it by the imposed ΔT.

Transverse Response

Figure 22 shows the macro transverse stress (Σ_T) and transverse strain ($\exists_T$), at room temperature, assuming perfect bonding between materials and accounting for the residual stresses developed during cooldown from fabrication. In addition to the three systems under consideration, that is, F/M, F/Cu/M, and F/Nb/M, the limiting cases of pure fiber and pure matrix are also shown. As one might expect, from knowing the CTE's of the matrix and fiber, the matrix–only case has the largest amount of residual strain, whereas the fiber–only case, has the least. Furthermore, it is clear from figure 22 that the initial stiffness and yield stress of the F/M system are increased over that of the matrix only response because of the presence of the fibers. Thus when a strong bond is achieved and maintained, the transverse response of the F/M system is greater than that of the matrix alone.

The inclusion of a Cu interface (see figure 22) gives an initial response very similar to that of the matrix alone, but insertion of a Nb interface gives an initial response similar to that of the F/M system. This indicates that the Cu interface is extremely successful in isolating (disconnecting) the fiber and matrix whereas the Nb has little success. Yet, after approximately 0.5% transverse strain the overall response of both interface systems is similar, and both responses appear to be softer than the F/M system (by approximately 22 %) because of the lower yield stress of the interfaces. They are, however, still stiffer than the matrix material alone, as a result of the presence of a strong bond.

Since debonding between fiber and matrix is known to occur under transverse loading when the SCS–6 fiber is used in a titanium based matrix, the above calculations were repeated with the assumption that no bond exist between the fiber and nonfiber materials; that is, the interface supports no tensile stress and assumes no frictional resistance. The results are shown in figure 23, where now the stress–strain response for all three composite systems falls far short of the matrix–only behavior, and, as before, both interface systems give a response that is softer than the F/M–alone response. Here, however, as one might expect because of the reduction in residual radial clamping stress, the F/Cu/M system experiences the onset of debonding first, and it is followed by the F/Nb/M and F/M systems. Note that both the F/Nb/M and F/M system apparently debond at the same macro stress level; however, the F/M bond has opened less than that of

the F/Nb/M, which indicates that if a smaller increment in load were applied, a different macro stress that causes debonding could be determined for the F/Nb/M system.

CONCLUDING REMARKS

The present study investigated the influence of two types of engineered interfaces (i.e., compliant and compensating layers) on the development of thermal residual stresses (due to fabrication) and the mechanical response (due to subsequent subjection to either a thermal or mechanical load) in a SiC/Ti_3Al+Nb composite system. The representative compliant layer chosen for this system was Nb, whereas the representative compensating layer was Cu. The stress analysis results were obtained by using the nonlinear finite element program MARC and two different finite element models. The first, an elastic–plastic axisymmetric concentric cylinder model that does not account for any surrounding fiber interaction, was employed to investigate the thermal response of the composite. The second, a three–dimensional elastic–plastic unit cell model with periodic boundary conditions representing a hexagonally packed composite architecture, was employed to analyze the mechanical response of the various composite systems.

Results indicate that, overall, the compensating layer interface reduced thermal residual stresses within the fiber and matrix while increasing the ductility at the interface, whereas the compliant layer increased the fiber and matrix stresses as well as the ductility at the interface. The degree of impact that either type of interface might have was shown to depend on the thickness of the layer as well as the fiber volume fraction.

In particular, the influence of a compensating layer was shown to be significantly more sensitive to the thickness of the layer and the fiber volume fraction than the influence of a compliant layer. For example, as the thickness of the compensating layer increased, the in–plane stress and the strain range within the matrix decreased while that within the interface itself increased. The importance of this thickness dependence was illustrated even more clearly when multiple layers were present (see fig. 10) and such dependence suggests that there is significant flexibility for designing a layered system that not only will reduce thermal stresses within the matrix (to a desired level) but also will control the increase in stresses within the interface itself. Such a design would prolong the life of an interface subjected to thermal cycling.

Application of a longitudinal mechanical load after cooldown showed that the presence of either a compensating or complaint layer interface had only a minor influence on the longitudinal tensile response. Alternatively, application of a transverse load produced a slight decrease in the transverse stiffness of the composite systems with an interface, as compared to the system without an interface. Also it has been shown, as one

might expect, that when debonding is permitted, the presence of a compensating layer will lower the macro transverse stress required to initiate debonding, because of the reduction in residual radial clamping on the fiber. Furthermore, it has been shown that if a strong bond is present, the composite response will be stiffer than that of the matrix itself, but if no bond is present, the response will be less than that of the matrix alone.

In the future, the authors will analyze the thermal–mechanical response of such composite systems as those presented here, by mapping out their respective shakedown, ratcheting, and cyclic plasticity zones. Currently, these systems are being manufactured and experimentally tested so as to verify and illuminate the previous as well as present numerical results.

REFERENCES

1. Brindley P.K.; Bartolotta P.A.; and MacKay, R.A.: Thermal and Mechanical Fatigue of SiC/Ti_3Al + Nb Composite. HITEMP Review 1989: Advanced High Temperature Engine Materials Technology Program, NASA CP–10039, 1989, pp. 52–1 to 52–14.

2. Arnold, S. M.; Arya, V.K.; and Melis M.E.: Elastic/Plastic Analysis of Advanced Composites Investigating the Use of The Compliant Layer Concept in Reducing Residual Stresses Resulting from Processing. NASA TM–103204, 1990.

3. Arnold, S. M.; Arya, V.K.; and Melis M.E.: Reduction of Thermal Residual Stresses in Advanced Metallic Composites Based Upon A Compensating/ Compliant Layer Concept. To appear in J. Compos., 1992.

4. Misra, A.K.; and Arnold, S.M.: Compliant Layer For The Ti_3Al+Nb/SCS–6 Composite System. NASA TM–105344, 1991.

5. Misra, A.K.: Chemical Compatibility Issues Related to Use of Copper as an Interfacial Layer for SiC Fiber Reinforced Ti_3Al+Nb Composite. NASA CR–187100, 1991.

6. Doghri, I.; and Leckie, F.A.: Elasto–Plastic Analysis of Interface Layers for Fiber Reinforced Metal Matrix Composites. NASA CR–187133, 1991.

7. Misra, A.: Private Communication, Materials Division, NASA Lewis Research Center, Cleveland, OH.

8. MARC, Revision K.3. MARC Analysis Research Corporation, Palo Alto, CA, 1988.

9. Brindley, P.K., et al.: Factors Which Influence Tensile Strength of a SiC/Ti–24Al–11Nb Composite. Fundamental Relationships Between Microstructures and Mechanical Properties of Metal Matrix Composites, Proceedings of the Symposium, TMS Fall Meeting, M.N. Gungor and P.K. Liaw, eds., ASM, 1990, pp. 387–401.

10. Brindley, P.K., et al.: The Effect of Temperature on The Deformation and Fracture of SiC/Ti–24Al—11Nb . To be published in Metall. Trans. A., 1992.

11. Internal Documentation. Textron Specialty Inc, Lowell, Mass.

12. Stuart, H., ed.: Niobium, Proceedings of the International Symposium, The Metallurgical Society of ATME, Warrendale, PA, 1981.

13. American Society for Metals: Properties and Selection: Nonferrous Alloys and Pure Metals/Metals Handbook. Ninth ed., Vol 2, ASM, 1979.

14. Freed, A.D.: Thermoviscoplastic Model With Application to Copper. NASA TP–2845, 1988.

15. Chen, W.F.; and Han, D.J.: Plasticity For Structural Engineers. Springer–Verlag, 1988.

16. McClintock, F.A.; and Argon, A.J.: Mechanical Behavior of Materials. Addison–Wesley, 1966.

17. Manson, S.S.: Fatigue: A Complex Subject – Some Simple Approximations. Exp. Mech., vol. 5, no. 7, July 1965, pp. 193–226.

18. Draper, S.L.; Brindley, P.K.; and Nathal M.V.: Effects of Fiber Strength on the Room Temperature Tensile Properties of SiC/Ti–24Al–11Nb. To be published in Metall. Trans. A., 1992.

Table I.–Experimentally Obtained Temperature-Dependent Fiber and Matrix Material Parameters

(a) Fiber (SiC; SCS-6)
[Poisson's ratio = 0.25.]

Temperature, °C	Coefficient of thermal expansion, α, in./in./°C	Modulus of elasticity, E, GPa
25	3.53×10^{-6}	400
101	3.56	↓
203	3.62	
300	3.73	
400	3.87	
500	4.03	
598	4.19	
702	4.35	
800	4.46	
900	4.59	

(b) Matrix (Ti-24Al-11Nb)
[Poisson's ratio = 0.26.]

Temperature, °C	Material property			
	Coefficient of thermal expansion α, in./in./°C	Modulus of elasticity, E, GPa	Yield stress, σ_y, MPa	Hardening slope ratio,[a] H/H_o
23	9.00×10^{-6}	110	372	1.0
200	9.36	100	372	.1323
425	10.26	75.8	370	.0966
600	10.53	86.2	291	.056
650	10.62	68.2	270	.0291
815	11.07	42.7	165	0

[a]H_o = 22.98 GPa.

Table II.–Niobium (Nb) Temperature-Dependent Material Properties[a]
[Poisson's ratio = 0.38.]

Temperature, °C	Material property		
	Coefficient of thermal expansion α, in./in./°C	Modulus of elasticity, E, GPa	Yield stress, σ_y, MPa
25	7.13×10^{-6}	98.6	248
140	7.24	96.5	214
300	7.36	93.8	186
456	7.49	89.6	138
600	7.61	87.6	82.7
800	7.77	82.7	75.8
1000	7.92	79.3	60.0

[a]Hardening slope ratio has the same temperature dependence as Cu (see table III), but with H_o = 1/4 H_o of Cu.

Table III.–Copper (Cu) Temperature-Dependent Material Properties Used in Stress Analysis
[Poisson's ratio = 0.34.]

Temperature, °C	Material property			
	Coefficient of thermal expansion α, in./in./°C	Modulus of elasticity, E, GPa	Yield stress, σ_y, MPa	Hardening slope ratio,[a] H/H_o
23	16.0×10^{-6}	78.8	37.1	1.0
204	17.0	58.9	31.6	.670
427	18.36	36.8	26.6	.3733
649	19.25	24.0	22.5	.1817
760	19.8	16.8	20.0	.1534
871	20.36	12.1	19.2	.128
982	20.92	10.3	19.2	.078

[a]H_o = 6.374 GPa.

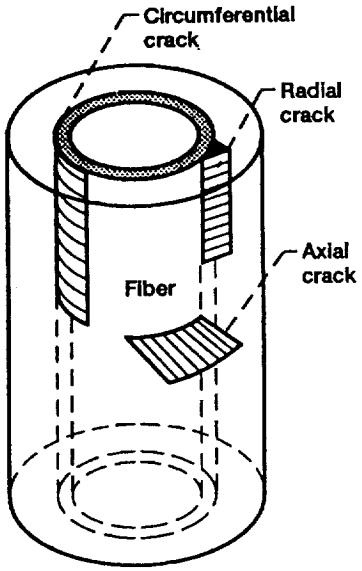

Figure 1.—Possible internal crack orientations.

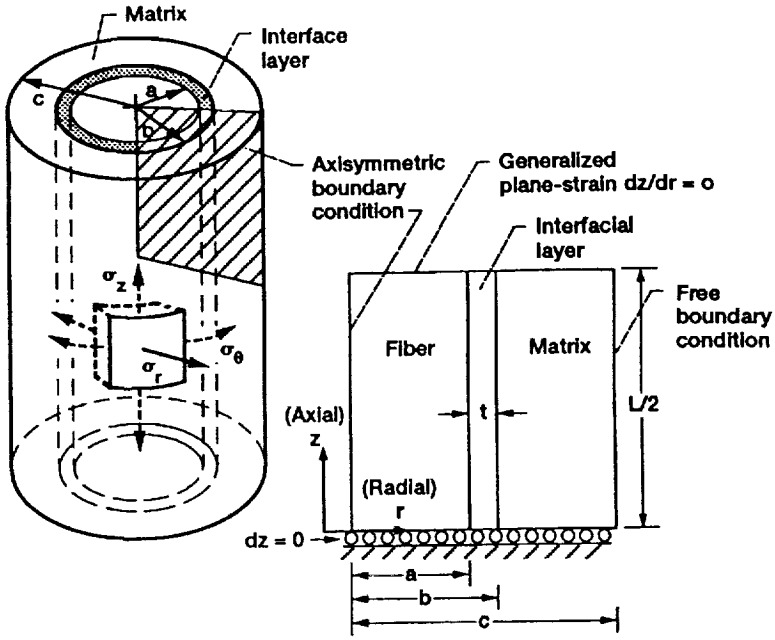

Figure 2.—Concentric cylinder model and FEA boundary condition.

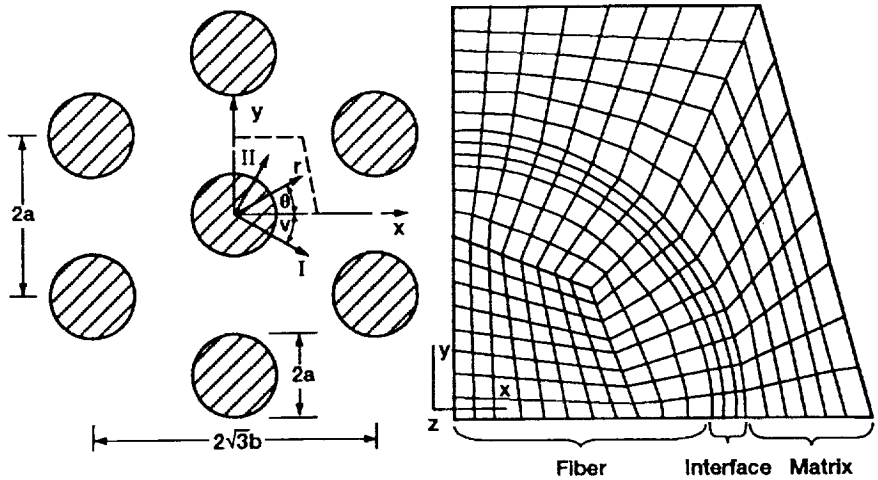

(a) Hexagonal array with unit cell indicated. (b) Finite element mesh.

Figure 3.—Three-dimensional unit cell model with periodic boundary conditions representing hexagonal packing.

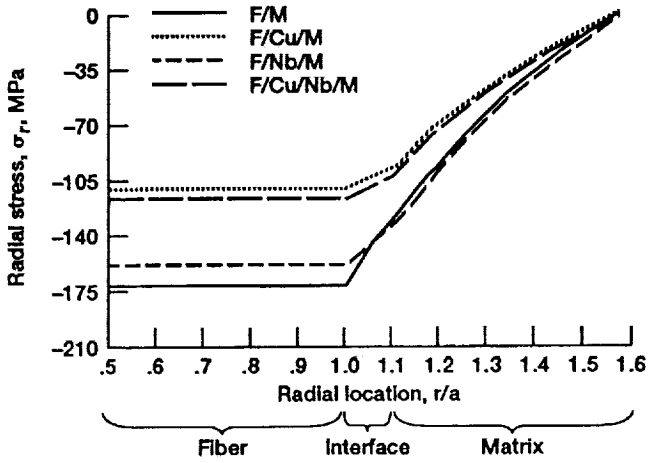

Figure 4.—Residual radial stress versus radial location for F/M system and the F/Cu/M, F/Nb/M, and F/Cu/Nb/M systems, each with total interface thickness t/a = 0.1.

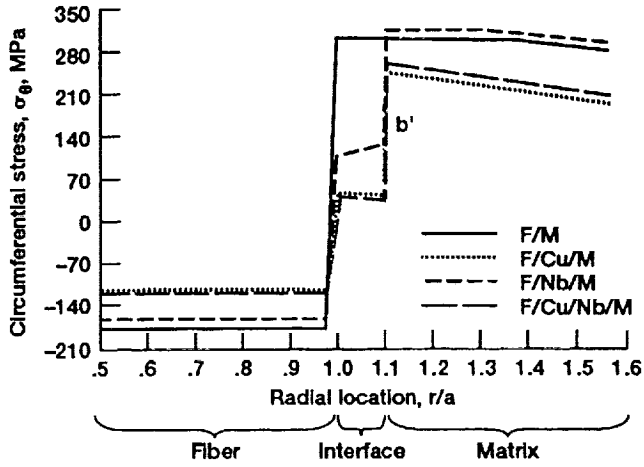

Figure 5.—Residual circumferential stress versus radial location for F/M system and the F/Cu/M, F/Nb/M, and F/Cu/Nb/M systems, each with total interface thickness t/a = 0.1.

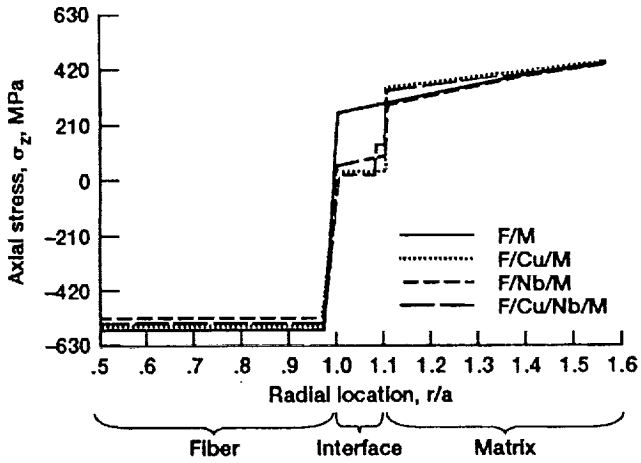

Figure 6.—Residual axial stress versus radial location for F/M system and the F/Cu/M, F/Nb/M, and F/Cu/Nb/M systems, each with total interface thickness t/a = 0.1.

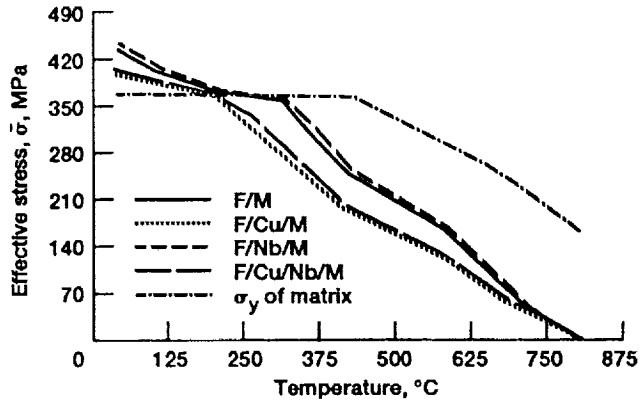

Figure 7.—Effective stress versus temperature in the Ti_3Al+Nb matrix material, illustrating the onset of plasticity.

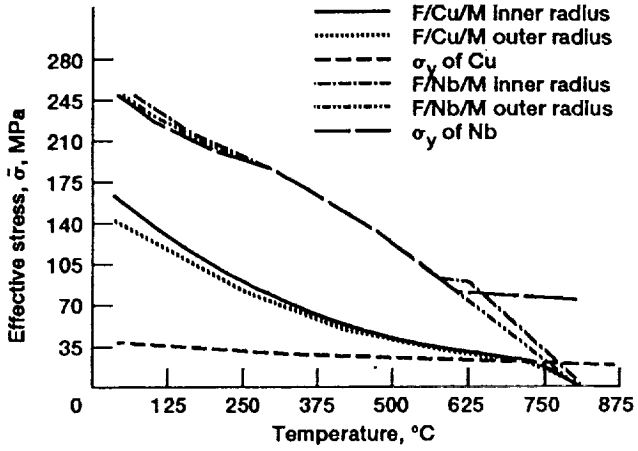

Figure 8.—Effective stress versus temperature in Cu and Nb interface material, illustrating onset of plasticity.

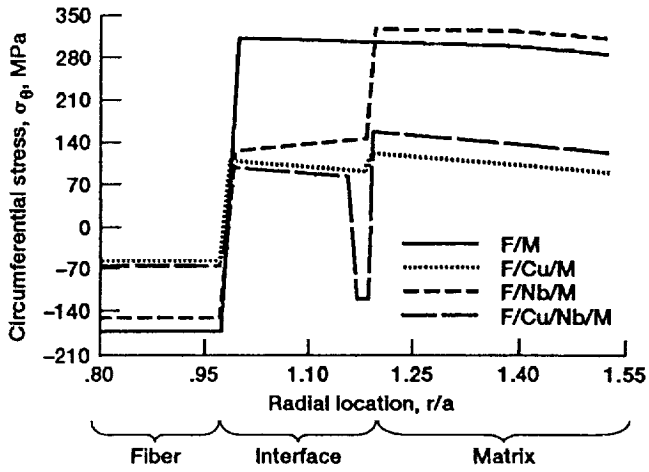

Figure 9.—Residual circumferential stress versus radial location for F/M system and the F/Cu/M, F/Nb/M, and F/Cu/Nb/M systems, each with total interface thickness t/a = 0.2.

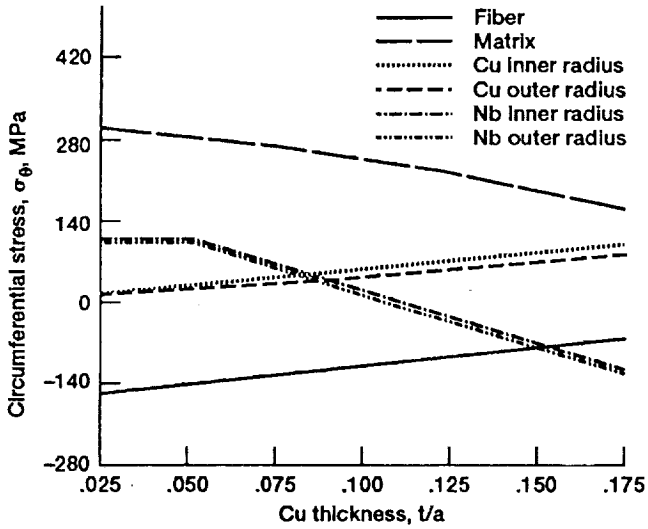

Figure 10.—Effect on circumferential stress of increasing thickness of inner compensating layer (Cu) while thickness of diffusion barrier (Nb) is held constant at t/a = 0.05.

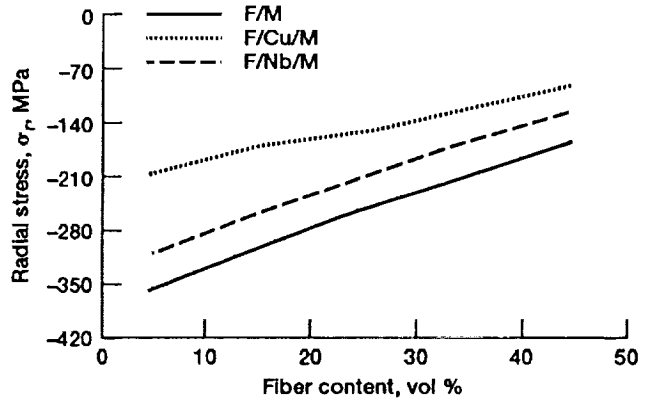

Figure 11.—Effect of fiber volume fraction on thermal residual stress in radial direction, at location b' in the matrix, after cooldown to room temperature.

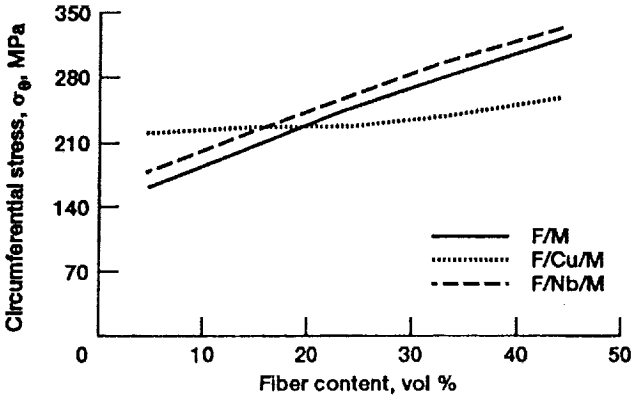

Figure 12.—Effect of fiber volume fraction on thermal residual stress in circumferential direction, at location b' in the matrix, after cooldown to room temperature.

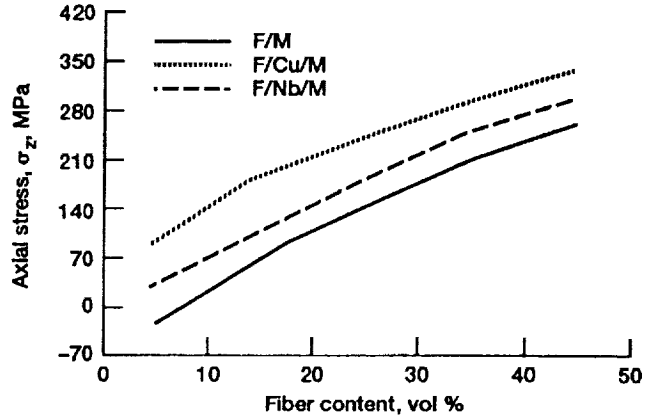

Figure 13.—Effect of fiber volume fraction on thermal residual stress in axial direction, at location b' in the matrix, after cooldown to room temperature.

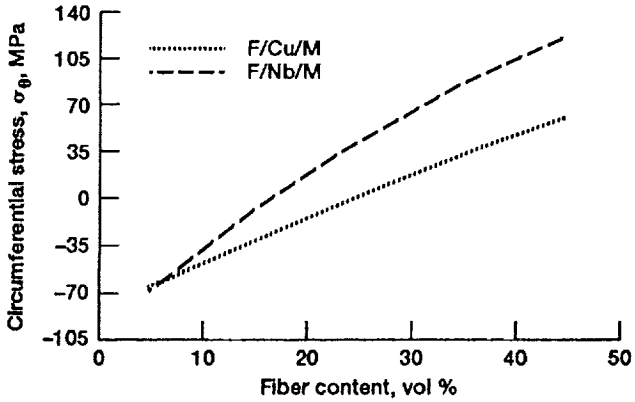

Figure 14.—Effect of fiber volume fraction on thermal residual stress in circumferential direction, at inner radius of the interface (t/a = 0.1), after cooldown to room temperature.

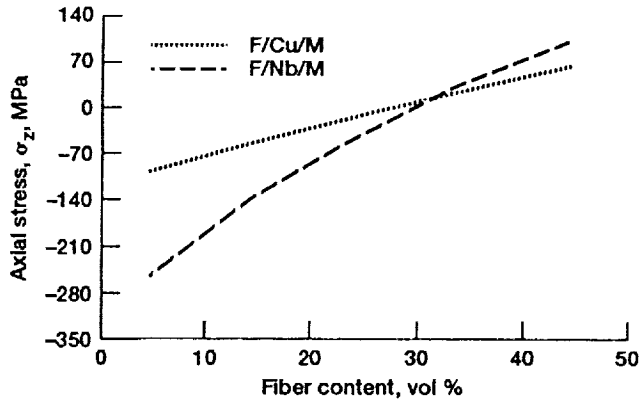

Figure 15.—Effect of fiber volume fraction on thermal residual stress in axial direction, at inner radius of the interface (t/a = 0.1), after cooldown to room temperature.

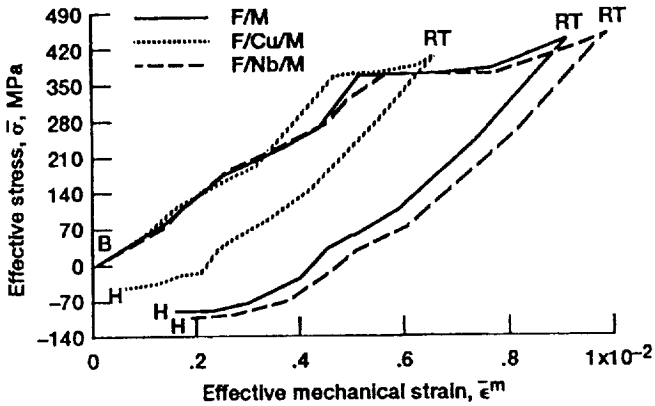

Figure 16.—Effective stress-mechanical strain history, at location b' in the matrix, for one thermal cycle from the initial stress-free temperature. Material response shown applies whether a kinematic or isotropic hardening model is assumed.

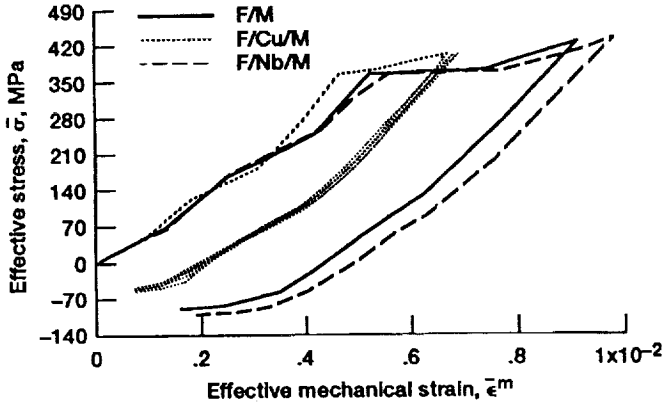

Figure 17.—Effective stress-mechanical strain history, at location b' in the matrix, for three complete thermal cycles, starting from the initial stress-free temperature and assuming isotropic hardening of both matrix and interface.

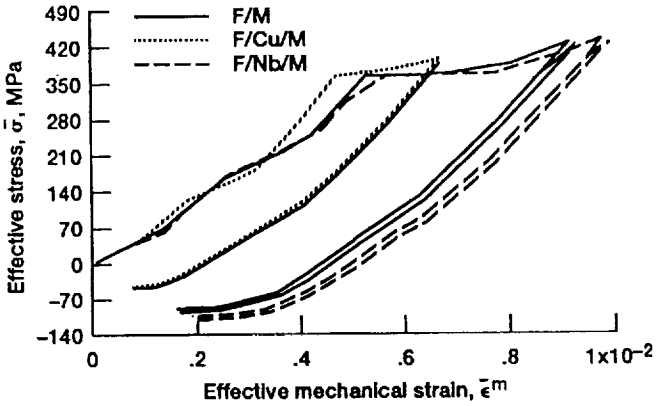

Figure 18.—Effective stress-mechanical strain history, at location b' in the matrix, for three complete thermal cycles, starting from the initial stress-free temperature and assuming kinematic hardening of both matrix and interface.

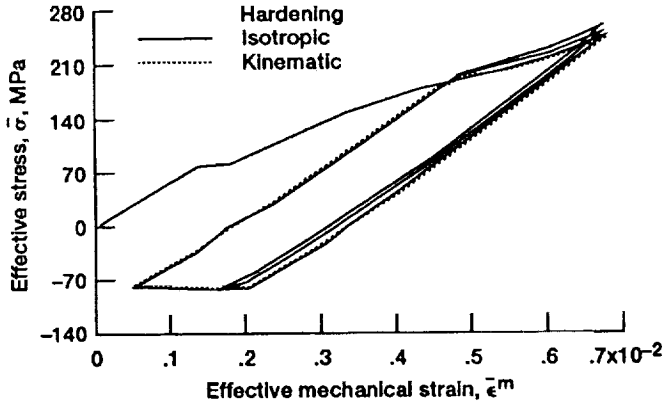

Figure 19.—Effective stress-mechanical strain history, at inner radius of the Nb interface, for three complete thermal cycles, starting from the initial stress-free temperature.

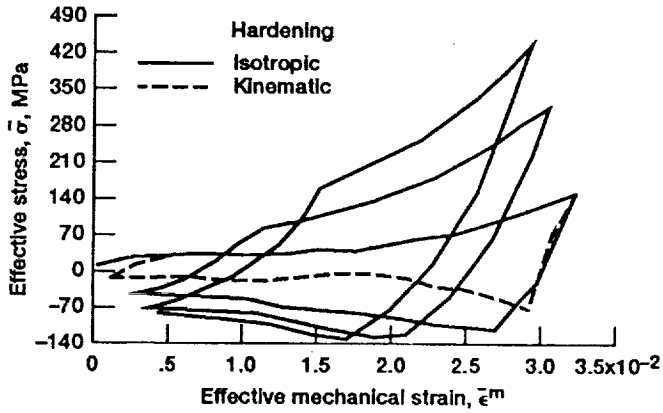

Figure 20.—Effective stress-mechanical strain history, showing both isotropic and kinematic hardening response at inner radius of Cu interface, for three complete thermal cycles starting from the initial stress-free temperature.

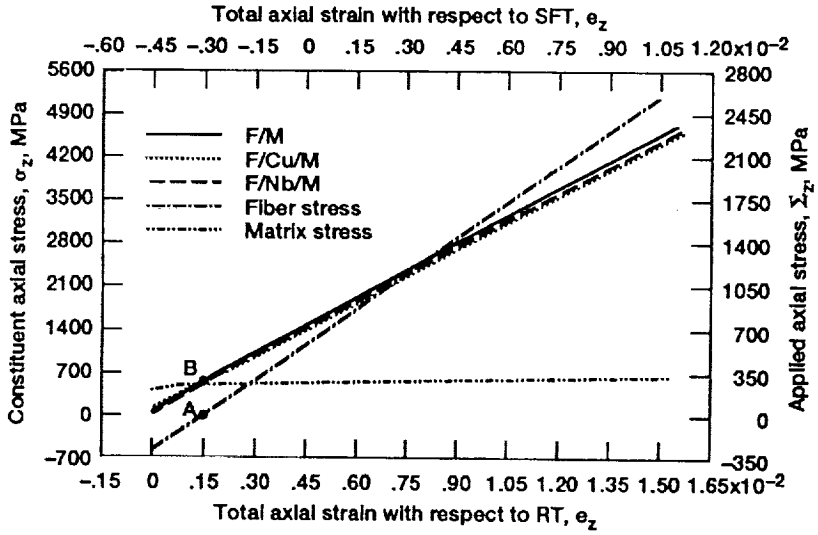

Figure 21.—Longitudinal tensile response of three composite systems subsequent to cooldown from initial stress-free temperature (SFT) to room temperature (RT). The fiber and matrix constituent axial stress-strain response is also shown.

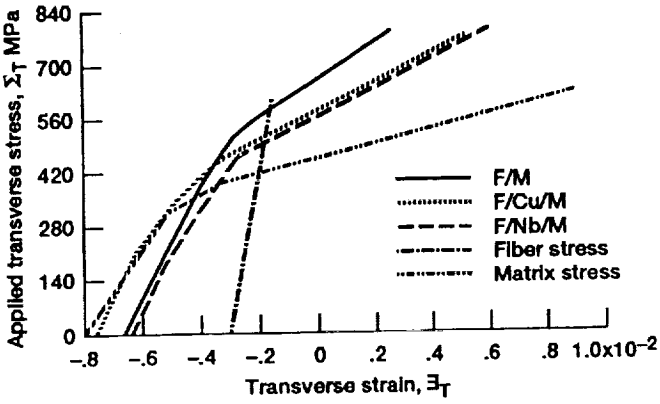

Figure 22.—Transverse tensile response of three composite systems, as well as fiber and matrix constituent, subsequent to cooldown from the initial stress-free temperature. Perfect bonding at the interface is assumed.

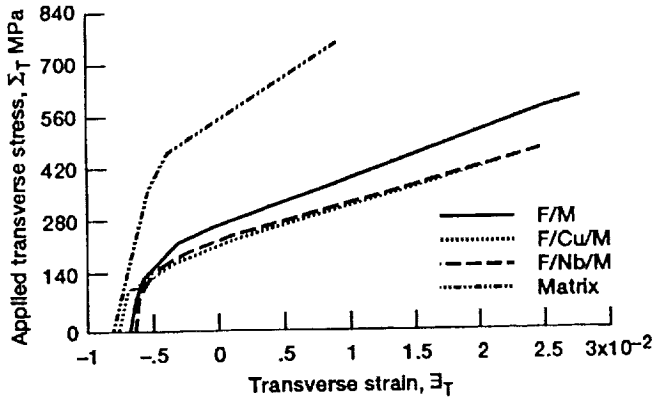

Figure 23.—Transverse tensile response of three composite systems, along with matrix-only response, subsequent to cooldown from the initial stress-free temperature. This assumes no bond at the fiber/nonfiber interface.

REPORT DOCUMENTATION PAGE

Form Approved
OMB No. 0704-0188

1. AGENCY USE ONLY (Leave blank)	2. REPORT DATE	3. REPORT TYPE AND DATES COVERED
	March 1992	Technical Memorandum

4. TITLE AND SUBTITLE

Influence of Engineered Interfaces on Residual Stresses and Mechanical Response in Metal Matrix Composites

5. FUNDING NUMBERS

WU-510-01-50

6. AUTHOR(S)

Steven M. Arnold and Thomas E. Wilt

7. PERFORMING ORGANIZATION NAME(S) AND ADDRESS(ES)

National Aeronautics and Space Administration
Lewis Research Center
Cleveland, Ohio 44135-3191

8. PERFORMING ORGANIZATION REPORT NUMBER

E-6866

9. SPONSORING/MONITORING AGENCY NAMES(S) AND ADDRESS(ES)

National Aeronautics and Space Administration
Washington, D.C. 20546-0001

10. SPONSORING/MONITORING AGENCY REPORT NUMBER

NASA TM-105438

11. SUPPLEMENTARY NOTES

Similar to material prepared for the Fourth International Conference on Composite Interfaces sponsored by Case Western Reserve University, Cleveland, Ohio, May 26-29, 1992. Steven M. Arnold, NASA Lewis Research Center; Thomas E. Wilt, University of Toledo, Toledo, Ohio 43606. Responsible person, Steven M. Arnold, (216) 433-3334.

12a. DISTRIBUTION/AVAILABILITY STATEMENT

Unclassified - Unlimited
Subject Categories 24 and 39

12b. DISTRIBUTION CODE

13. ABSTRACT *(Maximum 200 words)*

Because of the inherent coefficient of thermal expansion (CTE) mismatch between fiber and matrix within metal and intermetallic matrix composite systems, high residual stresses can develop under various thermal loading conditions. These conditions include cooling from processing temperature to room temperature as well as subsequent thermal cycling. As a result of these stresses, within certain composite systems, radial, circumferential, and/or longitudinal cracks have been observed to form at the fiber-matrix interface region. A number of potential solutions for reducing this thermally induced residual stress field have been proposed recently. Examples of some potential solutions are high CTE fibers, fiber preheating, thermal anneal treatments and an engineered interface (e.g., a compensating/compliant layer concept or a graded layer concept). In the strict sense, an engineered interface is one that provides a compromise between the various pertinent chemistry and mechanics issues for the application and the system under consideration. Here, the focus is on designing an interface (by using a compensating/compliant layer concept) to reduce or eliminate the thermal residual stress field and, therefore, the initiation and propagation of cracks developed during thermal loading. Furthermore, the impact of the engineered interface on the composite's mechanical response when subjected to isothermal mechanical load histories is examined.

14. SUBJECT TERMS

Residual stress; Elastic-plastic; Thermal stress; Metal matrix composites; Interfaces; Design

15. NUMBER OF PAGES

28

16. PRICE CODE

A03

17. SECURITY CLASSIFICATION OF REPORT	18. SECURITY CLASSIFICATION OF THIS PAGE	19. SECURITY CLASSIFICATION OF ABSTRACT	20. LIMITATION OF ABSTRACT
Unclassified	Unclassified	Unclassified	